Effect of pressure on the polarized infrared optical response of the quasi-one-dimensional conductor LaTiO$_{3.41}$

S. Frank and C. A. Kuntscher*

1. Physikalisches Institut, Universität Stuttgart, Pfaffenwaldring 57, D-70550 Stuttgart, Germany

I. Loa and K. Syassen

Max-Planck-Institut für Festkörperforschung, Heisenbergstrasse 1, D-70569 Stuttgart, Germany

F. Lichtenberg

Experimentalphysik VI, Institut für Physik, EKM, Universität Augsburg, Universitätsstrasse 1, D-86135 Augsburg, Germany

The pressure-induced changes in the optical properties of the quasi-one-dimensional conductor LaTiO$_{3.41}$ were studied by polarization-dependent midinfrared microspectroscopy at room temperature. For the polarization of the incident radiation parallel to the conducting direction, the optical conductivity spectrum shows a pronounced midinfrared absorption band, exhibiting a shift to lower frequencies and an increase in oscillator strength with increasing pressure. On the basis of its pressure dependence, interpretations of the band in terms of electronic transitions and polaronic excitations are discussed. Distinct changes in the optical response near 15 GPa are in agreement with a recently reported pressure-induced structural phase transition and indicate the onset of a dimensional crossover in this highly anisotropic system.

I. INTRODUCTION

Perovskite-related titanates are intensively studied both experimentally and theoretically, since they show interesting physical properties due to the complex interplay of structural and electronic degrees of freedom. Recently, special attention was paid to the compounds RTiO$_{3.0}$ (with R being a trivalent rare-earth ion),[1] which are Mott-Hubbard insulators with a Ti $3d^1$ configuration. LaTiO$_{3.0}$, in particular, has attracted much attention,[1–11] partly because of different orbital ordering scenarios. LaTiO$_{3.0}$ is the end member of the series LaTiO$_{3.5−x}$ with $0 \leq x \leq 0.5$, in which one finds a rich variety of different structural, magnetic, and electronic properties, depending on the composition parameter x. Besides the Mott-Hubbard system LaTiO$_{3.0}$, the band insulator LaTiO$_{3.5}$ is a prominent member of the series because of its ferroelectricity up to extremely high temperatures.[12]

Other compounds of the series LaTiO$_{3.5−x}$ were synthesized recently,[13] among them LaTiO$_{3.41}$, which is a quasi-one-dimensional (quasi-1D) conductor according to its anisotropic dc resistivity and infrared response.[13,14] It crystalizes in a monoclinic structure (space group $P2_1/c$) with lattice parameters a=7.86 Å, b=5.53 Å, c=31.48 Å, and β=97.1°.[15] The structure consists of slabs of vertex-sharing TiO$_6$ octahedra separated by additional oxygen layers (see Fig. 1). Along c the slabs are five octahedra wide, and neighboring slabs are shifted along the a axis by half an octahedron. The octahedra are tilted away from the a axis and rotated around this axis, similarly to the GdFeO$_3$-type arrangement of octahedra in LaTiO$_{3.0}$.[4] LaTiO$_{3.41}$ can thus be viewed as being built of LaTiO$_{3.0}$-type slabs. The characteristic units of the crystal structure are chains of TiO$_6$ octahedra, connected via their apical oxygen atoms and oriented along the a axis. These chains can serve as an explanation for the anisotropic electronic transport properties of

LaTiO$_{3.41}$, with relatively low resistivity values along the chain direction a.[13]

To shed light on the conduction mechanism of quasi-1D conducting LaTiO$_{3.41}$ its polarization-dependent reflectivity was studied as a function of temperature.[14] An anisotropic optical response was observed, with a Drude contribution of free carriers for the polarization of the incident radiation parallel to the conducting crystal axis a and an insulating character for the perpendicular direction b. Furthermore, the **E**$\|a$ optical conductivity spectrum includes a pronounced midinfrared (MIR) absorption band, showing a shift to lower frequencies and an increase in oscillator strength with decreasing temperature. A polaronic model was proposed to account for the temperature dependence of the MIR band.[14]

The application of external pressure to LaTiO$_{3.41}$ up to P=18 GPa leads to continuous changes of the crystal structure:[16] The axial compressibilities are anisotropic with a ratio of approximately 1:2:3 for the a, b, and c axes. The large compressibility along c results from the highly compressible oxygen-rich layers separating the LaTiO$_{3.0}$-type slabs (see Fig. 1). The differences in axis compressibilities cause a small increase of the monoclinic angle from 97.17° to 97.43° with increasing pressure up to 18 GPa. From the pressure dependence of the lattice parameters the octahedral tilt angle against the a axis was estimated to double at 18 GPa compared to ambient conditions. Above 18 GPa the appearance of additional reflections in the x-ray diffraction diagrams indicate a sluggish structural phase transition, which is completed at 24 GPa.[16]

In this paper we report the effect of pressure on the MIR reflectivity of LaTiO$_{3.41}$. Reflectivity spectra of a single-crystal sample were measured for polarizations along the a and b axes using MIR microspectroscopy in combination with a diamond anvil high pressure cell. The primary motivation is twofold: (1) Pressure effects are of considerable
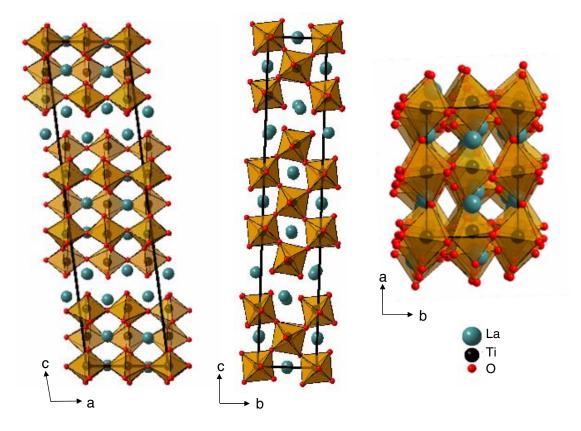
FIG. 1. (Color online) Crystal structure of LaTiO$_{3.41}$ composed of perovskitelike slabs of vertex-sharing TiO$_6$ octahedra, which are separated by additional oxygen layers (Ref. 15). Along the *a* axis the TiO$_6$ octahedra are connected via their apical oxygen atoms forming chains.

interest for the interpretation of the MIR band polarized along the conducting crystal direction. (2) In view of the anisotropic compressibility, external pressure is a means to continuously tune the electronic anisotropy in the *ab* plane and to explore the possibility of a crossover from one-to two-dimensional behavior. A further question is whether the pronounced optical anisotropy of the ambient-pressure phase is preserved across the first-order structural phase transition near 18 GPa.

II. EXPERIMENT

The investigated LaTiO$_{3.41}$ crystals were grown by a floating zone melting process, and their oxygen content was determined by thermogravimetric analysis.[13] Pressure-dependent reflectance measurements for the electrical field vector **E** of the incident light along the *a* and *b* axes were performed in the MIR frequency range (600–8000 cm^{-1}) at room temperature, using a Bruker IFs 66v/S Fourier transform infrared spectrometer. The measurements were carried out partly at the University of Stuttgart and partly at the infrared beamline of the synchrotron radiation source ANKA in Karlsruhe. A diamond anvil cell equipped with type IIA diamonds suitable for infrared measurements was used to generate pressures up to 20 GPa. To focus the infrared beam onto the small sample in the pressure cell, a Bruker IR Scope II infrared microscope with a 15× magnification objective was used. A field stop of 0.6 mm diameter was chosen,

which yields a geometrical spot size of 40 μm on the sample (diffraction effects neglected). The LaTiO$_{3.41}$ crystal was polished to a thickness of $\approx$40 μm. The reflectivity of the free-standing polished sample was checked and found to be in good agreement with earlier results.[14] A small piece of sample (about 80×80 μm^2) was cut and placed in the hole (150 μm diameter) of a steel gasket. Finely ground KCl powder was added as a quasihydrostatic pressure-transmitting medium. This solid but relatively soft medium ensures direct contact between the sample and the diamond anvil throughout the experiment. At 2 GPa, KCl undergoes a phase transition with a large volume reduction that helps to remove shear stresses introduced during the loading. In our experience KCl provides reasonably hydrostatic pressure conditions up to 20 GPa. The ruby luminescence method[17] was used for the pressure determination.

Polarized reflectivity spectra were measured at the interface between sample and diamond. The measurement geometry is shown in the inset of Fig. 2(b). Spectra taken at the inner diamond-air interface of the empty cell served as the reference for normalization of the sample spectra. The absolute reflectivity at the sample-diamond interface, denoted as R_{s-d}, was calculated according to $R_{s-d}(\omega)=R_{\mathrm{dia}} \times I_s(\omega)/I_d(\omega)$, where $I_s(\omega)$ denotes the intensity spectrum reflected from the sample-diamond interface and $I_d(\omega)$ the reference spectrum of the diamond-air interface. R_{dia} was calculated from the refractive index of diamond n_{dia} to 0.167 and assumed to be independent of pressure. This is justified
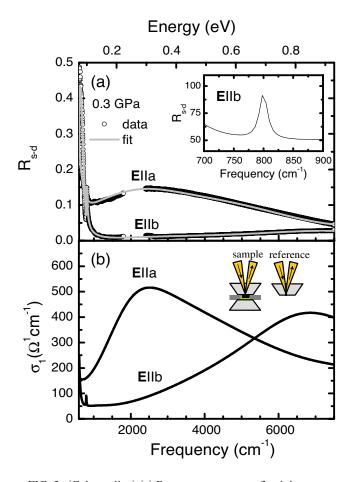
FIG. 2. (Color online) (a) Room-temperature reflectivity spectra R_{s-d} of LaTiO$_{3.41}$ inside the diamond anvil cell at $P=0.3$ GPa for the polarizations $\mathbf{E}\|a$ and $\mathbf{E}\|b$. The light gray lines are fits of the reflectivity spectra with the Drude-Lorentz model, taking into account the sample-diamond interface. Inset: Enlargement of the low-frequency range of the $\mathbf{E}\|b$ reflectivity spectrum showing the optical phonon mode at 800 cm^{-1}. (b) Optical conductivity spectra obtained from the Drude-Lorentz fits of the reflectivity data shown in (a). Inset: Geometries for the sample and reference measurements.

because n_{dia} is known to change only very little with pressure ($\Delta n_{\mathrm{dia}}/\Delta P=-0.00075$/GPa).[18,19] Variations in synchrotron source intensity were taken into account by applying additional normalization procedures. Strain-induced depolarization in the diamond anvil is considered negligible in the pressure range covered in the present experiment.

III. RESULTS

The reflectivity spectra of LaTiO$_{3.41}$ for the lowest pressure (0.3 GPa) are shown in Fig. 2(a) for $\mathbf{E}\|a,b$. The region around 2000 cm^{-1} is cut out from the experimental spectra since the diamond multiphonon absorption causes artifacts in this range. The overall reflectivity of the sample in the diamond anvil cell is lower than that of the free-standing sample[14] due to the smaller refractive index step at the sample-diamond interface.

The optical conductivity was obtained by fitting the reflectivity spectra with a Drude-Lorentz model combined with the normal-incidence Fresnel equation

$$R_{s-d} = \left| \frac{n_{\mathrm{dia}} - \sqrt{\epsilon_s}}{n_{\mathrm{dia}} + \sqrt{\epsilon_s}} \right|^2, \quad \epsilon_s = \epsilon_\infty + \frac{i\sigma}{\epsilon_0 \omega}, \quad (1)$$

where ϵ_s is the complex dielectric function of the sample. With the 15$\times$ objective used in the experiment, the angle of incidence of the radiation at the diamond-sample interface ranges from 4.1° to 9.5°; the average deviation from normal incidence is thus small enough to assume normal incidence for the data analysis. Furthermore, an increase of the background dielectric constant (by 14.5% at maximum) according to the Clausius-Mossotti relation[20] was assumed in the Drude-Lorentz fits to account for the pressure-induced reduction of the unit cell volume.[16]

As an example, we present in Fig. 2(a) the Drude-Lorentz fits of the reflectivity spectra for the lowest applied pressure (0.3 GPa); the resulting real part σ_1 of the optical conductivity is shown in Fig. 2(b) for both studied polarizations. For fitting the lowest-pressure data, the fitting parameters for the reflectivity spectra of the free-standing sample were used as starting parameters. The resulting optical conductivity spectra at 0.3 GPa [Fig. 2(b)] are in overall agreement with the ambient-pressure results.[14]

For the polarization of the radiation parallel to the conducting axis a the optical conductivity spectrum consists of a pronounced, asymmetric absorption band, located at around 2500 cm^{-1} at 0.3 GPa. For the perpendicular polarization direction, $\mathbf{E}\|b$, a phonon mode located at 800 cm^{-1} and a broadband centered around 7000 cm^{-1} are observed for the lowest applied pressure.

The polarization-dependent reflectivity spectra R_{s-d} for pressures up to $\approx$20 GPa are presented in Fig. 3. Features around $\omega=2500$ and 3700 cm^{-1} are artifacts originating from multiphonon absorptions of diamond which are not fully corrected by the normalization procedure. For $\mathbf{E}\|a$ the reflectivity increases continuously with increasing pressure in the whole frequency range studied here. In contrast, for $\mathbf{E}\|b$ the overall reflectivity is almost unchanged up to a pressure of $\approx$15 GPa and only above 15 GPa R_{s-d} increases strongly. Furthermore, the phonon mode located at 800 cm^{-1} in the $\mathbf{E}\|b$ spectrum hardens with increasing pressure [for spectra see inset of Fig. 3(b)]. In Fig. 4 the peak position of the phonon mode is shown as a function of applied pressure: Up to 15 GPa the mode hardens in a linear fashion with a pressure coefficient of 3.2 ± 0.5 cm^{-1}/GPa; at around 15 GPa a discontinuous change in the frequency of the observed spectral feature occurs.

The pressure-dependent real part σ_1 of the optical conductivity obtained from the Drude-Lorentz fits is presented in Fig. 5. With increasing pressure the MIR band observed in the $\mathbf{E}\|a$ optical conductivity shifts to lower frequencies and its oscillator strength increases. This MIR band is superimposed by a relatively narrow peak at $\approx$1200 cm^{-1}, whose oscillator strength strongly increases above 15 GPa. For the polarization $\mathbf{E}\|b$ gradual changes set in at $\approx$10 GPa. With increasing pressure the absorption band located at around
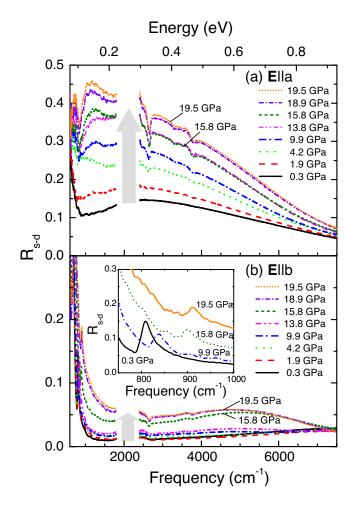
FIG. 3. (Color online) Room-temperature reflectivity spectra R_{s-d} of LaTiO$_{3.41}$ as a function of pressure for the polarization (a) $\mathbf{E}\|a$ and (b) $\mathbf{E}\|b$. The inset in (b) shows the low-frequency range (700–1000 cm^{-1}) of the spectra for four pressures. The phonon at around 800 cm^{-1} shifts to higher frequencies with increasing pressure. The arrows indicate the changes with increasing pressure.
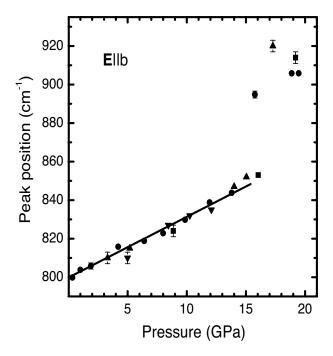

FIG. 4. Peak position of the phonon mode measured for $\mathbf{E}\|b$. Different symbols are used for different experimental runs. Up to 14 GPa the mode hardens in a linear fashion, with a linear pressure coefficient of 3.2 cm^{-1}/GPa. The line is a linear fit of the data points. At around 15 GPa an abrupt change in the frequency of the vibrational feature occurs.

7000 cm^{-1} for the lowest pressure looses oscillator strength and the spectral weight moves to the frequency range 4000–5000 cm^{-1}. A massive redistribution of spectral weight occurs between 14 and 16 GPa. Furthermore, at around ≈15 GPa a significant increase of the optical conductivity in the low-frequency part (<2000 cm^{-1}) of the $\mathbf{E}\|b$ spectrum is observed.

Upon releasing pressure, the pressure-dependent trends, e.g., overall increase of reflectivity for $\mathbf{E}\|a$, the sudden change in frequency of the $\mathbf{E}\|b$ phonon mode, and the redistribution of spectral weight in the high frequency range, are reversible.

IV. DISCUSSION

A. Low-pressure regime: $P<15$ GPa

In the low-pressure regime ($P<15$ GPa) the changes in the optical response with increasing pressure are continuous. In the $\mathbf{E}\|b$ optical conductivity spectrum there is a small

redistribution of the high-frequency spectral weight near ≈7000 cm^{-1} towards lower frequency. That spectral weight may be due to charge transfer excitations, and the pressure-induced redistribution may reflect subtle alterations in the crystal structure,[16] causing changes in the electronic band structure.

For $\mathbf{E}\|a$ one finds a monotonic redshift and spectral weight growth of the pronounced MIR band with increasing pressure. Based on Drude-Lorentz fits of the reflectivity spectra, the contribution of the MIR band to the optical conductivity was extracted. The zero crossing of the first derivative of this contribution served as an estimate for the frequency position of the band. The so-obtained position of the $\mathbf{E}\|a$ MIR band is plotted in Fig. 6 as a function of applied pressure. In addition, we show the pressure dependence of its spectral weight which increases by a factor of 2 for pressures up to 20 GPa.

Based on its absolute strength and pressure dependence, the MIR band can be interpreted in terms of (i) excitations of purely electronic character and (ii) excitations involving electron-phonon coupling, i.e., polaronic excitations.

For the interpretation of the MIR band in terms of purely electronic excitations, it is instructive to compare the ambient-pressure spectrum of LaTiO$_{3.41}$ with that of the Mott-Hubbard insulator LaTiO$_{3.0}$. For LaTiO$_{3.0}$ the increase of the optical conductivity at around 700 cm^{-1} is due to excitations from the lower to the upper Hubbard band.[21–25] Upon hole doping, additional excitations within the Mott-Hubbard gap were theoretically predicted[26,27] and experimentally demonstrated:[23,24,28] namely, a coherent Drude term
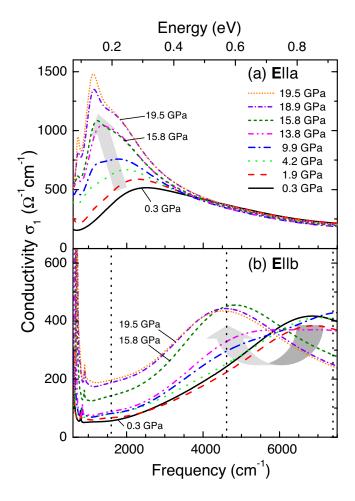
FIG. 5. (Color online) Pressure-dependent real part of the optical conductivity of LaTiO$_{3.41}$ for (a) $\mathbf{E}\|a$ and (b) $\mathbf{E}\|b$ at room temperature, obtained by Drude-Lorentz fitting of the reflectivity data. The arrows indicate the changes with increasing pressure. The dotted vertical lines in (b) indicate the frequency positions analyzed in Fig. 7.

FIG. 6. Frequency position (closed squares) and spectral weight (open triangles) of the $\mathbf{E}\|a$ MIR band as a function of pressure. Dashed lines are guides to the eye.

and an incoherent MIR band due to transitions between the quasiparticle peak at the Fermi energy to the upper Hubbard band (or from the lower Hubbard band to the quasiparticle peak).

In analogy, assuming a Mott-Hubbard picture, LaTiO$_{3.41}$ with an electronic configuration $3d^{0.18}$ is in a highly hole-doped regime, and the $\mathbf{E}\|a$ MIR band could be attributed to the predicted incoherent innergap excitations. The observed pressure-induced redshift and spectral weight growth of the MIR band reminds one of the doping- or thermally induced changes of the incoherent MIR band in Mott-Hubbard systems.[29] Accordingly, the pressure-induced effects in LaTiO$_{3.41}$ could be attributed to the bandwidth-controlled delocalization of charges.

It is interesting to compare the crystal structure of LaTiO$_{3.41}$ with that of the Mott-Hubbard system LaTiO$_{3.0}$.[4] At ambient conditions, the crystal structure of LaTiO$_{3.0}$ is of the orthorhombic GdFeO$_3$-type with characteristic tiltings and distortions of the TiO$_6$ octahedra. The Ti-O1 bond length and Ti-O1-Ti bond angle (with O1 denoting the apex oxygen ion) influence the $3d$ electron bandwidth,[28] and amount to
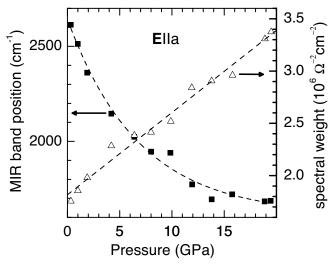
2.03 Å and 154°, respectively.[4] A three-dimensional network of tilted and distorted TiO$_6$ octahedra is also present in LaTiO$_{3.41}$ within an (a,b)-slab. Each slab consists of five chains of TiO$_6$ octahedra along the a axis and connected via their apical oxygen ions. Within a slab, the octahedral tiltings and distortions are not homogeneous, but the largest average Ti-O1-Ti bond angle (163°) and smallest average Ti-O1 bond length (1.99 Å) are present within the chain at the symmetrical position in the middle of the slab. Interestingly, in LaTiO$_{3.0}$ a pressure-induced insulator-to-metal transition is observed for Ti-O1 bond lengths just below 2 Å.[30] This suggests that in LaTiO$_{3.41}$ the central chains within the slabs play a key role for the observed conducting properties of this compound.

The other scenario for the interpretation of the pronounced asymmetric $\mathbf{E}\|a$ MIR absorption band of LaTiO$_{3.41}$ is in terms of an optical signature of polaronic quasiparticles that are formed due to electron-phonon interaction.[31] Within a polaronic picture, the frequency position of the MIR band is a measure of the polaronic binding energy and thus of the electron-phonon coupling strength. Such a MIR absorption band was found in several well-studied materials, like cuprates,[32–36] manganites,[37–39] and nickelates.[32,37,40,41] Also several titanium oxides show the characteristic absorption feature of polarons in the MIR frequency range,[42–46] and also for LaTiO$_{3.41}$ such a picture had been suggested to explain the pronounced MIR band for $\mathbf{E}\|a$.[14]

For the manganites it was demonstrated that the MIR band is very sensitive to the application of chemical or external pressure, see, e.g., Refs. 47–49. In the case of doped manganites,[48,49] pressure effects were attributed to tuning the strength of the electron-phonon coupling and thus the extent of the localization of the charges. In general, a broadening of the electronic bands, i.e., an enhancement of the electron itineracy, and a stiffening of the lattice is expected upon pressure application. As a consequence, the electron-phonon coupling and therefore the polaronic binding energy should decrease. So a shift of the MIR band to lower energies and
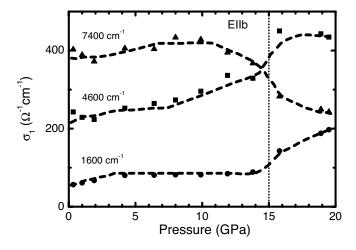
FIG. 7. Real part of the **E**∥*b* optical conductivity at three different frequencies (1600, 4600, and 7400 cm⁻¹) as a function of pressure (extracted from Fig. 5). The dotted vertical line indicates the pressure where the structural phase transition reported earlier (Ref. 16) occurs in the present optical study. Dashed lines are guides to the eye.

an increase of the oscillator strength, indicating an enhanced delocalization of the charge carriers, are then expected. This is in agreement with the observed pressure-induced changes of the MIR absorption feature in LaTiO$_{3.41}$ [see Figs. 5(a) and 6].

Thus, based on the pressure dependence of the MIR band it is difficult to draw a conclusion on the question whether this absorption feature is to be explained by a Mott-Hubbard or a polaronic scenario. For both the Mott-Hubbard and the polaron model several examples exist, where the distinct doping dependences of the spectral features were demonstrated.[23,28,34,36,40] Thus, also in the case of the titanate LaTiO$_{3.41}$ the doping dependence of the MIR absorption band might be an important additional piece of information. Further insight could be obtained by a detailed line shape analysis of the absorption band.

B. High-pressure regime: $P > 15$ GPa

Near 15 GPa we observe distinct changes in the optical response: (i) The oscillator strength of the narrow peak superposing the MIR band for the polarization **E**∥*a* increases. (ii) For **E**∥*b* a pronounced redistribution of spectral weight from high (≈ 7400 cm⁻¹) to lower (≈ 4600 cm⁻¹) frequencies occurs, indicating the shift of the broad **E**∥*b* excitation band. (iii) There is a sudden change in frequency of the vibrational excitation showing up in the MIR spectra (see Fig. 4). (iv) In the low-frequency part ($\omega < 2000$ cm⁻¹) the optical conductivity perpendicular to the chains, **E**∥*b*, remains almost constant in the lower pressure range, and starts to increase above ≈ 15 GPa (see changes at 1600 cm⁻¹ illustrated in Fig. 7).

These discontinuities are most probably related to the pressure-induced structural phase transition, which was observed at 18 GPa by x-ray diffraction measurements under more hydrostatic conditions.[16] Such an offset in pressure of

the induced changes for different pressure transmitting media was already observed in other experimental studies.[50,51] Due to the large number of overlapping reflections, the high-pressure crystal structure could not be determined; a reversible distortion of the low-pressure crystal structure was suggested.[16] According to our optical data, the structural transition affects both the vibrational and electronic excitations of the system. Above the phase transition, i.e., for $P > 15$ GPa, the broad **E**∥*b* excitation band is located at ≈ 5000 cm⁻¹ and remains almost unchanged when increasing the pressure.

The pronounced increase of the low-frequency part ($\omega < 2000$ cm⁻¹) of the optical conductivity spectrum *perpendicular* to the chains (**E**∥*b*) deserves special attention. It cannot be simply explained by the redshift of the higher-lying broad band. An additional oscillator below 2000 cm⁻¹ needs to be included to describe the high-pressure (i.e., $P > 15$ GPa) reflectivity spectra with the Drude-Lorentz model. This suggests the onset of a pressure-induced dimensional crossover of the system at 15 GPa, i.e., a significant increase of the hopping integral perpendicular to the chains. However, the anisotropy of the material is preserved up to the highest applied pressure (19.5 GPa), since the overall optical conductivity for **E**∥*a* remains higher compared to **E**∥*b*.

V. SUMMARY

We studied the polarization-dependent midinfrared reflectivity of the quasi-1D conducting titanate LaTiO$_{3.41}$ as a function of pressure. Below 15 GPa the changes with increasing pressure are continuous for both polarizations studied: For **E**∥*a* the overall reflectivity increases; the corresponding optical conductivity contains a pronounced MIR absorption band showing a redshift and an increase of spectral weight with increasing pressure. Based on its pressure dependence, this MIR band can be interpreted in terms of electronic transitions within a Mott-Hubbard picture in the hole-doped regime, but the pressure-induced changes may also be consistent with an interpretation in terms of polaronic excitations. For **E**∥*b* almost no change in the reflectivity spectra is induced with increasing pressure up to 15 GPa; only a small redistribution of spectral weight towards lower frequencies is observed.

Near 15 GPa, distinct changes are clearly observed in the optical response. However, the optical anisotropy of the low-pressure phase persists in the regime of the high-pressure phase. This indicates a well-defined orientational relationship between low-pressure and high-pressure phases. The dominant change of the optical response at the phase transition occurs for **E**∥*b*: a pronounced redshift of the excitation band, a sudden change in frequency of the phonon mode, and an increase of the low-frequency optical conductivity. These changes can be related to the recently observed[16] pressure-induced structural phase transition, which alters the electronic band structure and induces the onset of a dimensional crossover in this highly anisotropic system.

ACKNOWLEDGMENTS

---

*Present address: Experimentalphysik II, Institut für Physik, Universität Augsburg, D-86159 Augsburg, Germany; email: christine.kuntscher@physik.uni-augsburg.de

[1] M. Mochizuki and M. Imada, New J. Phys. **6**, 154 (2004), and references therein.

[2] G. Khaliullin and S. Maekawa, Phys. Rev. Lett. **85**, 3950 (2000).

[3] B. Keimer, D. Casa, A. Ivanov, J. W. Lynn, M. v. Zimmermann, J. P. Hill, D. Gibbs, Y. Taguchi, and Y. Tokura, Phys. Rev. Lett. **85**, 3946 (2000).

[4] M. Cwik, T. Lorenz, J. Baier, R. Müller, G. André, F. Bourée, F. Lichtenberg, A. Freimuth, R. Schmitz, E. Müller-Hartmann, and M. Braden, Phys. Rev. B **68**, 060401(R) (2003).

[5] M. Mochizuki and M. Imada, Phys. Rev. Lett. **91**, 167203 (2003).

[6] J. Hemberger, H.-A. Krug von Nidda, V. Fritsch, J. Deisenhofer, S. Lobina, T. Rudolf, P. Lunkenheimer, F. Lichtenberg, A. Loidl, D. Bruns, and B. Büchner, Phys. Rev. Lett. **91**, 066403 (2003).

[7] T. Kiyama and M. Itoh, Phys. Rev. Lett. **91**, 167202 (2003).

[8] E. Pavarini, S. Biermann, A. Poteryaev, A. I. Lichtenstein, A. Georges, and O. K. Andersen, Phys. Rev. Lett. **92**, 176403 (2004).

[9] M. W. Haverkort, Z. Hu, A. Tanaka, G. Ghiringhelli, H. Roth, M. Cwik, T. Lorenz, C. Schüssler-Langeheine, S. V. Streltsov, A. S. Mylnikova, V. I. Anisimov, C. de Nadai, N. B. Brookes, H. H. Hsieh, H.-J. Lin, C. T. Chen, T. Mizokawa, Y. Taguchi, Y. Tokura, D. I. Khomskii, and L. H. Tjeng, Phys. Rev. Lett. **94**, 056401 (2005).

[10] R. Rückamp, E. Benckiser, M. W. Haverkort, H. Roth, T. Lorenz, A. Freimuth, L. Jongen, A. Möller, G. Meyer, P. Reutler, B. Büchner, A. Revcolevschi, S.-W. Cheong, C. Sekar, G. Krabbes, and M. Grüninger, New J. Phys. **7**, 144 (2005).

[11] C. Ulrich, A. Gössling, M. Grüninger, M. Guennou, H. Roth, M. Cwik, T. Lorenz, G. Khaliullin, and B. Keimer, cond-mat/0503106 (to be published).

[12] S. Nanamatsu, M. Kimura, K. Doi, S. Matsushita, and N. Yamada, Ferroelectrics **8**, 511 (1974).

[13] F. Lichtenberg, A. Herrnberger, K. Wiedenmann, and J. Mannhart, Prog. Solid State Chem. **29**, 1 (2001).

[14] C. A. Kuntscher, D. van der Marel, M. Dressel, F. Lichtenberg, and J. Mannhart, Phys. Rev. B **67**, 035105 (2003).

[15] P. Daniels, F. Lichtenberg, and S. van Smaalen, Acta Crystallogr., Sect. C: Cryst. Struct. Commun. **59**, i15 (2003).

[16] I. Loa, K. Syassen, X. Wang, F. Lichtenberg, M. Hanfland, and C. A. Kuntscher, Phys. Rev. B **69**, 224105 (2004).

[17] H. K Mao, J. Xu, and P. M. Bell, J. Geophys. Res., [Atmos.] **91**, 4673 (1986).

[18] M. I. Eremets and Y. A. Timofeev, Rev. Sci. Instrum. **63**, 3123 (1992).

[19] A. L. Ruoff and K. Ghandehari, in *High Pressure Science and Technology*, edited by S. C. Schmidt, J. W. Shaner, G. A. Samara, and M. Ross, AIP Conf. Proc. No. 309 (AIP, New York, 1994), pp. 1523–1525.

[20] N. W. Ashcroft and N. D. Mermin, *Solid State Physics* (Harcourt Brace College Publishers, Fort Worth, 1976).

[21] P. Lunkenheimer, T. Rudolf, J. Hemberger, A. Pimenov, S. Tachos, F. Lichtenberg, and A. Loidl, Phys. Rev. B **68**, 245108 (2003).

[22] T. Arima, Y. Tokura, and J. B. Torrance, Phys. Rev. B **48**, 17006 (1993).

[23] T. Katsufuji, Y. Okimoto, and Y. Tokura, Phys. Rev. Lett. **75**, 3497 (1995).

[24] Y. Okimoto, T. Katsufuji, Y. Okada, T. Arima, and Y. Tokura, Phys. Rev. B **51**, 9581 (1995).

[25] D. A. Crandles, T. Timusk, J. D. Garrett, and J. E. Greedan, Phys. Rev. B **49**, 16207 (1994).

[26] M. Jarrell, J. K. Freericks, and Th. Pruschke, Phys. Rev. B **51**, 11704 (1995).

[27] M. J. Rozenberg, G. Kotliar, and H. Kajueter, Phys. Rev. B **54**, 8452 (1996).

[28] Y. Taguchi, Y. Tokura, T. Arima, and F. Inaba, Phys. Rev. B **48**, 511 (1993).

[29] M. Imada, A. Fujimori, and Y. Tokura, Rev. Mod. Phys. **70**, 1039 (1998).

[30] I. Loa, K. Syassen, X. Wang, H. Roth, and T. Lorenz (unpublished).

[31] D. Emin, Phys. Rev. B **48**, 13691 (1993).

[32] X.-X. Bi and P. C. Eklund, Phys. Rev. Lett. **70**, 2625 (1993).

[33] J. P. Falck, A. Levy, M. A. Kastner, and R. J. Birgeneau, Phys. Rev. B **48**, 4043 (1993).

[34] P. Calvani, M. Capizzi, S. Lupi, P. Maselli, A. Paolone, and P. Roy, Phys. Rev. B **53**, 2756 (1996).

[35] S. Lupi, M. Capizzi, P. Calvani, B. Ruzicka, P. Maselli, P. Dore, and A. Paolone, Phys. Rev. B **57**, 1248 (1998).

[36] S. Lupi, P. Maselli, M. Capizzi, P. Calvani, P. Giura, and P. Roy, Phys. Rev. Lett. **83**, 4852 (1999).

[37] P. Calvani, A. Paolone, P. Dore, S. Lupi, P. Maselli, P. G. Medaglia, and S.-W. Cheong, Phys. Rev. B **54**, R9592 (1996).

[38] K. H. Kim, J. H. Jung, and T. W. Noh, Phys. Rev. Lett. **81**, 1517 (1998).

[39] Ch. Hartinger, F. Mayr, J. Deisenhofer, A. Loidl, and T. Kopp, Phys. Rev. B **69**, 100403(R) (2004).

[40] X.-X. Bi, P. C. Eklund, and J. M. Honig, Phys. Rev. B **48**, 3470 (1993).

[41] D. A. Crandles, T. Timusk, J. D. Garret, and J. E. Greedan, Physica C **216**, 94 (1993).

[42] V. N. Bogomolov and D. N. Mirlin, Phys. Status Solidi **27**, 443 (1968); V. N. Bogomolov, E. K. Kudinov, D. N. Mirlin, and Ju. A. Firsov, Sov. Phys. Solid State **9**, 1630 (1968).

[43] P. Gerthsen, R. Groth, K. H. Hardtl, D. Heese, and H. G. Reik, Solid State Commun. **3**, 165 (1965).

[44] D. M. Eagles and P. Lalousis, J. Phys. C **17**, 655 (1984).

[45] P. Calvani, M. Capizzi, F. Donato, S. Lupi, P. Maselli, and D. Peschiaroli, Phys. Rev. B **47**, 8917 (1993).

[46] V. V. Kabanov and D. K. Ray, Phys. Rev. B **52**, 13021 (1995).

[47] I. Loa, P. Adler, A. Grzechnik, K. Syassen, U. Schwarz, M. Hanfland, G. Kh. Rozenberg, P. Gorodetsky, and M. P. Pasternak, Phys. Rev. Lett. **87**, 125501 (2001).

[48] A. Congeduti, P. Postorino, P. Dore, A. Nucara, S. Lupi, S. Mercone, P. Calvani, A. Kumar, and D. D. Sarma, Phys. Rev. B **63**, 184410 (2001).

[49] P. Postorino, A. Congeduti, P. Dore, A. Sacchetti, F. Gorelli, L. Ulivi, A. Kumar, and D. D. Sarma, Phys. Rev. Lett. **91**, 175501 (2003).

[50] I. Loa, U. Schwarz, M. Hanfland, R. K. Kremer, and K. Syassen, Phys. Status Solidi B **215**, 709 (1999).

[51] I. Loa, A. Grzechnik, U. Schwarz, K. Syassen, M. Hanfland, and R. K. Kremer, J. Alloys Compd. **317-318**, 103 (2001).